Identification and Targeting of *POLQ*-Associated Hereditary Colorectal Cancer

Ning Xu[1,2], Deng-Feng Zhang[3], Xiao-Xiao Shi[4], Ke-Xin Yang[1], Bei-Bei Gan[1], Yu Fan[3], Feng-Chang Huang[2], Jun-Yu Ren[2], Rui Bi[3], Yu Li[3], Mao-Sen Ye[3], Min Xu[3], Yong-Chun Zhou[1], Wen-Hui Li[1], Yong-Gang Yao[3], and Wen-Liang Li[1,5]

ABSTRACT

Purpose: Hereditary colorectal cancer syndromes remain incompletely understood, with many cases lacking defined genetic causes. This study aimed to identify pathogenic mutations associated with hereditary colorectal cancer and explore their potential for targeted therapies.

Experimental Design: This observational study was conducted in Yunnan Province, China. We analyzed 43 individuals from 12 families with hereditary colorectal cancer using whole-exome sequencing, screened 84 families with polyposis and 310 sporadic colorectal cancer cases, and analyzed an expanded cohort of 285 individuals with potential hereditary colorectal cancer. A series of *in vivo* and *in vitro* assays were conducted to evaluate the mutation's effects on tumorigenesis.

Results: A germline heterozygous stop-gain mutation, p.Arg1953X in the polymerase θ (*POLQ*) gene, was identified in two families with colorectal cancer, showing cosegregation with disease status. A third *POLQ* mutation–positive family was identified in the expanded validation cohort. Cells carrying the mutation showed potential of tumorigenesis. The mutation hyperactivates error-prone θ-mediated end-joining (TMEJ), leading to high tumor mutational burden and resistance to DNA-damaging treatments. Indeed, the probands exhibited mismatch repair–deficient/microsatellite instability–high status that indicates high tumor mutational burden. Treatment with the *POLQ* inhibitor novobiocin suppressed TMEJ activity and restored tumor sensitivity to DNA damage, providing a combined medication scheme for drug-resistant *POLQ*-type colorectal cancer.

Conclusions: This study identifies *POLQ* as a pathogenic gene in hereditary colorectal cancer, unveiling a novel *POLQ*-type colorectal cancer driven by TMEJ hyperactivation. Screening for *POLQ* mutations in patients with hereditary adenomas or early-onset colorectal cancer would benefit early diagnosis and personalized therapy for *POLQ*-associated colorectal cancer; however, further clinical validation is warranted.

Introduction

Mendelian cancer syndromes account for approximately 5% of colorectal cancer cases (1), with Lynch syndrome (LS) being the most recognized, characterized by early-onset colorectal cancer or endometrial cancer, primarily due to defects in DNA mismatch repair (MMR; ref. 2). Other hereditary syndromes, such as familial adenomatous polyposis and *MUTYH*-associated polyposis, predispose individuals to multiple adenomas, which can serve as benign precursors to colorectal cancer (3, 4). Besides these well-recognized syndromes, multiple adenomas are also an important hallmark of hereditary colorectal cancer, yet the mechanisms underlying this phenotype remain poorly understood. These syndromes, along with rarer ones like juvenile polyposis syndrome and polymerase proofreading-associated polyposis, highlight the critical role of DNA repair in colorectal cancer prevention. Pathogenic genes involved in these processes include *MSH2*, *MLH1*, *MSH6*, and *PMS2* (MMR); *MUTYH* and *NTHL1* (base excision repair); and *POLD1* and *POLE* (proofreading repair), all of which maintain genomic stability and encode for key enzymes in DNA repair pathways. Research on these DNA repair pathways may provide potential therapeutic targets for cancer (5–8).

Despite these insights, the etiology of many hereditary colorectal cancer cases remains unclear, particularly in families presenting with polyposis but lacking known mutations. This suggests the presence of unidentified genetic contributors. Therefore, identifying these unknown genes and their underlying mechanisms and developing drugs that target these pathways is critical for these patients.

In this study, we initially investigated 12 hereditary families with colorectal cancer using whole-exome sequencing (WES). We identified a novel germline mutation in the *POLQ* gene (p.Arg1953X) that cosegregated with disease status, validated in two additional pedigrees. This study is the first to implicate *POLQ* in hereditary colorectal cancer or polyposis, revealing a new genetic pathway in colorectal cancer development. Additionally, we identified novobiocin (NVB),

[1]The Third Affiliated Hospital of Kunming Medical University, Yunnan Cancer Hospital, Peking University Cancer Hospital Yunnan, Kunming, China. [2]The First Affiliated Hospital of Kunming Medical University, Kunming, China. [3]State Key Laboratory of Genetic Evolution and Animal Models, Yunnan Key Laboratory of Animal Models and Human Disease Mechanisms, National Research Facility for Phenotypic & Genetic Analysis of Model Animals (Primate Facility), Kunming Institute of Zoology, Chinese Academy of Sciences, Kunming, China. [4]Yan'an Affiliated Hospital of Kunming Medical University, Kunming, China. [5]The Second Affiliated Hospital of Kunming Medical University, Kunming, China.

N. Xu and D.-F. Zhang contributed equally to this article.

Corresponding Authors: Wen-Liang Li, Department of Colorectal Surgery, The Third Affiliated Hospital of Kunming Medical University, Yunnan Cancer Hospital, Kunming, Yunnan 650100, China. E-mail: liwenliang@kmmu.edu.cn; and Deng-Feng Zhang, State Key Laboratory of Genetic Evolution and Animal Models, Kunming Institute of Zoology, Chinese Academy of Sciences, Kunming 650201, China. E-mail: zhangdengfeng@mail.kiz.ac.cn

Clin Cancer Res 2025;XX:XX–XX

doi: 10.1158/1078-0432.CCR-25-0379

Translational Relevance

This research identifies a previously unrecognized genetic driver, polymerase θ (*POLQ*), in hereditary colorectal cancer characterized by early-onset and multiple adenomas. The identification of the *POLQ* p.Arg1953X mutation in 3% of hereditary colorectal cancer pedigrees and its association with enhanced θ-mediated end-joining DNA repair, leading to resistance to standard treatments, is of critical clinical importance. The effectiveness of the *POLQ* inhibitor novobiocin in reversing this resistance suggests that *POLQ* and θ-mediated end-joining are promising therapeutic targets. The work supports the need for routine *POLQ* mutation screening in patients who present with multiple adenomas or early-onset colorectal cancer. By providing both a specific genetic marker and a novel targeted therapy, the research lays the foundation for more precise diagnosis and personalized treatment options of POLQ-associated colorectal cancer.

an FDA-approved drug, as a potential therapeutic option for *POLQ*-associated cancers, supported by both *in vitro* and *in vivo* analyses.

Materials and Methods

Ethics statement

All animal experiments and housing were conducted in strict accordance with the institutional guidelines for the care and use of laboratory animals and were approved by the Institutional Animal Care and Use Committee of Kunming Medical University (approval no. KMMU20221009). For studies involving human participants, the protocol was reviewed and approved by the Institutional Review Board of Kunming Medical University (approval no. 2017-3), and written informed consent was obtained from all participants prior to enrollment. All procedures involving human participants were conducted in accordance with the Declaration of Helsinki.

Study design and patient cohorts

This observational study aimed to identify genetic mutations associated with hereditary colorectal cancer in Han Chinese families from Yunnan Province, China. In the discovery phase, 12 families with hereditary colorectal cancer, characterized by multiple primary tumors (especially colorectal cancer and adenomas), early-onset colorectal cancer or adenomas (before age 50), and a family history of related cancers, were selected. These families exhibited two phenotypes: polyposis and nonpolyposis colorectal cancer. Probands were evaluated for LS and enrolled at least two affected individuals and one healthy control who underwent WES, leading to the identification of a germline *POLQ* p.Arg1953X mutation in the LS7 family with a polyposis phenotype.

In the validation phase, the study was expanded to include 84 additional families with polyposis and 310 sporadic colorectal cancer cases. The prevalence of the *POLQ* p.Arg1953X mutation was assessed using Sanger sequencing, with population data obtained from the gnomAD database for East Asians. As part of the validation phase, an expanded whole-genome sequencing (WGS) cohort of 285 individuals from Yunnan with potential hereditary colorectal cancer, characterized by early-onset colorectal cancer, multiple polyps, and/or a family history of colorectal cancer (not limited to families with polyposis), was included.

Sequencing and genotyping

Whole exome of probands and their family members ($N = 43$, sequenced individuals are shown in **Fig. 1A** and Supplementary Fig. S1A) were captured using Agilent SureSelect Human All Exon V6 Kit. WES data processing was performed following the best practice recommendations of GATK (https://gatk.broadinstitute.org/). The WES-identified *POLQ* mutation in the LS7 family was verified using standard Sanger sequencing, and all members within the LS7 family were also sequenced. During the verification phase, Sanger sequencing was used to detect the *POLQ* p.Arg1953X mutation, with one known mutation and one wild-type (WT) sample included as the control in each run. For the LS13 family carrying the *POLQ* p.Arg1953X mutation, Sanger sequencing was extended to other family members. WES was used to exclude known pathogenic gene mutations in this family. For the expanded WGS cohort, WGS was performed to detect the *POLQ* p.Arg1953X mutation. The family member of the *POLQ* mutation–positive case was also reviewed for clinical information.

Analysis of tumor mutational burden and microsatellite instability status

The colorectal cancer tumors from one affected member each of the LS7 (I:2) and LS13 (II:2) families, along with 320 individuals without the *POLQ* p.Arg1953X mutation, underwent genomic profiling of 769 cancer-related genes. Genomic DNA was extracted from blood (for germline mutation) and formalin-fixed, paraffin-embedded tumor samples (for somatic mutation). Libraries were prepared using a capture-based method and sequenced on an Illumina platform. Data were processed with standard bioinformatics pipelines, using Mutect2, VarScan2, and Pindel for calling variants.

Tumor mutational burden (TMB) was calculated as nonsynonymous somatic mutations per megabase (Mb) of exonic regions. Tumors were classified as high-TMB if they had more than 10 mutations/Mb and low-TMB if they had 10 or fewer mutations/Mb.

Microsatellite instability (MSI) status was assessed using 55 microsatellite loci from NGS data. Samples were classified as MSI-high (MSI-H) if more than 20% of loci were unstable, MSI-low if 10% to 20% were unstable, and microsatellite stable if fewer than 10% were unstable. MSI was validated using IHC and pentaplex PCR with five markers (BAT25, BAT26, D5S346, D17S250, and D2S123). Tumors with two or more unstable markers were MSI-H, and those with stable markers were microsatellite stable.

WGS and somatic mutation pattern analysis of *POLQ*-mutated cells

We conducted WGS of $POLQ^{+/R1953X}$ HCT116 cells to investigate the pattern of somatic mutations obtained in *POLQ*-mutated cells. Somatic variants were called for WGS data using TNseq from Sentieon Genomics software (bioRxiv 115717) following procedures described in the software manuals (https://support.sentieon.com/versions/201808.03/manual/TNseq_usage), which matches the GATK's Mutect2 somatic variant calling pipelines. Briefly, WGS data of each sample were mapped to the human reference genome (GRCh38) using Burrows-Wheeler Aligner (9), followed by duplication removal, insertion/deletion (indel) realignment, and base quality score recalibration. To generate a panel of normal samples,

germline and somatic variants were first called for each replicate of WT cells using the TNhaplotyper algorithm referred to COSMIC mutations (https://cancer.sanger.ac.uk/cosmic/, coding and non-coding mutations; ref. 10) and dbSNP138. The generated VCF files (accessible at http://mitotool.kiz.ac.cn/lab/download/HCT116_WT_POLQ_WGS.tar) from all WT samples were then merged using bcftools (11). Mutations with allele count >1 were kept and used as the reference panel. For each replicate from the WT and mutant (MUT) groups, somatic variants were called using the TNhaplotyper algorithm referred to the panel of normal samples, COSMIC mutations, and dbSNP138. Somatic mutational catalogs were generated using SigProfilerMatrixGenerator (12). SBS96, ID83, and DBS78 catalogs were generated for each sample, and the matrices were subsequently fitted to COSMIC signatures (v3.4) using R package deconstructSigs (13).

Vector construction and transfection

Myc- and Flag-tagged *POLQ* expression plasmids were obtained from Addgene (#73132). The p.Arg1953X mutation was created using the Easy Mutagenesis System (TransGen Biotech) and confirmed by Sanger sequencing (Supplementary Table S1).

Transient transfection was done with Lipofectamine 3000 (Invitrogen). Cells were seeded in six-well plates and, at 50% to 60% confluency, washed with Opti-MEM (Gibco). Vectors (2.5 μg/well) were mixed with P3000 reagent and Lipofectamine 3000 in Opti-MEM. After a 15-minute incubation, the mixture was added to each well. After 6 hours, the medium was replaced with fresh growth medium. Cells were harvested 48 hours after transfection.

Cell lines and reagents

For functional assays, we utilized HEK293T (RRID: CVCL_0063) and HCT116 (RRID: CVCL_0291) cell lines to investigate the impact of the *POLQ* p.Arg1953X mutation. The HEK293T cell line was chosen due to its well-established use in gene editing and overexpression studies, providing a robust system for assessing the functional consequences of specific mutations in a well-defined genetic background. Furthermore, 293T cells exhibit proficient nonhomologous end-joining (NHEJ), a pathway in which *POLQ* plays a significant role, making them a suitable cellular context for measuring *POLQ* mutation–related effects on this repair mechanism. In addition to HEK293T, the HCT116 cell line was used to provide complementary insights and cross-validation. The HCT116 cell line, a MMR-deficient (MLH1-deficient) colorectal cancer cell line, offers a relevant context for evaluating the impact of *POLQ* mutations within a cancer cell background in which genomic instability is already present. By using both cell lines, we aimed to gain a more comprehensive understanding of the role of *POLQ* in different DNA repair contexts and how MMR status may influence *POLQ* function.

The primary antibodies and chemicals used in this study are listed in Supplementary Table S2. The HEK293T and HCT116 cell lines were obtained from Kunming Cell Bank (Kunming Institute of Zoology) and cultured in DMEM (Thermo Fisher Scientific) supplemented with 10% FBS (Thermo Fisher Scientific) at 37°C in 5% CO_2. All cell lines were authenticated using short tandem repeat profiling by Kunming Cell Bank. *Mycoplasma* contamination was routinely tested using a PCR-based method (Myco-Lumi Luminescent Mycoplasma Detection Kit, Beyotime), and all cell lines tested negative. Etoposide and NVB were dissolved in DMSO at an appropriate concentration as a stock solution and stored at −80°C before further use.

Genome editing of HEK293T and HCT116 cell lines

We generated *POLQ* p.Arg1953X knock-in cell lines using a CRISPR/Cas9-mediated homologous recombination (HR) approach, as described in our previous study (14). Cells were cotransfected with the px330-mCherry vector (Addgene #98750) and single-stranded oligonucleotides designed to introduce the specific mutations (Supplementary Table S1). At 48 hours after transfection, mCherry-positive cells were sorted by flow cytometry, followed by single-cell clone expansion. The clones were then genotyped using Sanger sequencing to confirm successful incorporation of the mutations.

For the p.Gln1949X mutation, a similar CRISPR/Cas9-based base-editing method was used using the same guide RNA designed for *POLQ* p.Arg1953X. The cells were cotransfected with pCMV-BE4 (Addgene #100802) for base editing, and puromycin selection was applied to isolate edited clones. Successful base editing was verified through sequencing.

For *POLQ* knockout (KO) in HCT116 cells, we used CRISPR/Cas9 with guide RNAs targeting exon regions of the *POLQ* gene (Supplementary Table S1). After transfection and puromycin selection, single-cell clones were isolated, expanded, and confirmed for KO by Sanger sequencing and Western blotting to ensure the absence of *POLQ* protein.

Cell viability and colony formation assays

Cell viability was assessed using Cell Counting Kit-8 (CCK-8, Beyotime). Cells were seeded in 96-well plates at 1,000 cells/well. CCK-8 substrate (10 μL) was added on days 0, 1, 2, 3, 4, and 5 after treatment and incubated at 37°C for 2 hours. Absorbance was measured at 450 nm.

For colony formation, cells were seeded in six-well plates at 500 cells/well. Colonies were counted using ImageJ after fixing with methanol and staining with Giemsa solution (Beyotime). The surviving fraction was calculated as the ratio of treated to control plating efficiency.

DNA synthesis assay

To detect the DNA synthesis of mutated cells under stress, BeyoClick EdU Cell Proliferation Kit was used with Alexa Fluor 647 (Beyotime C0080L) according to the manufacturer's protocols. Briefly, cells were seeded in 12-well plates at 1×10^4 cells/well in 1 mL of standard medium, alone or with ionizing radiation (IR; 6 Gy). After 24 hours, the cells were incubated with 10 μmol/L 5-ethynyl-2′-deoxyuridine (EdU) in conditioned medium for 2 hours, followed by fixing, permeabilizing, and staining. For each sample, at least 10 random fields were observed by fluorescence microscopy, and mean gray values were counted.

Apoptosis assay by flow cytometry

An annexin V-FITC/propidium iodide (PI; 556547, BD Biosciences) apoptosis staining assay was performed to detect cell apoptosis. In brief, 2×10^5 cells were collected using trypsin without EDTA. After twice washing with PBS, cells were incubated in the dark with 500 μL of binding buffer, 5 μL of annexin V-FITC, and 10 μL of PI for 10 minutes at room temperature. Fluorescence intensity of samples was quantified by flow cytometry (BD FACSCanto II; BD Biosciences). Experiments were carried out in triplicate.

Cell-cycle analysis

Cells were seeded in 12-well plates at 50% to 60% confluence and treated as indicated 24 hours after plating. The cells were then

harvested at 0, 6, and 24 hours after DNA damage induction. After fixing in 70% ice-cold ethanol overnight, the cells were then stained with PI in the presence of RNase A (Beyotime C1052). Fluorescence intensity was measured by flow cytometry. The percentages of cells in the G0/G1, S, and G2/M phases were analyzed using FlowJo software.

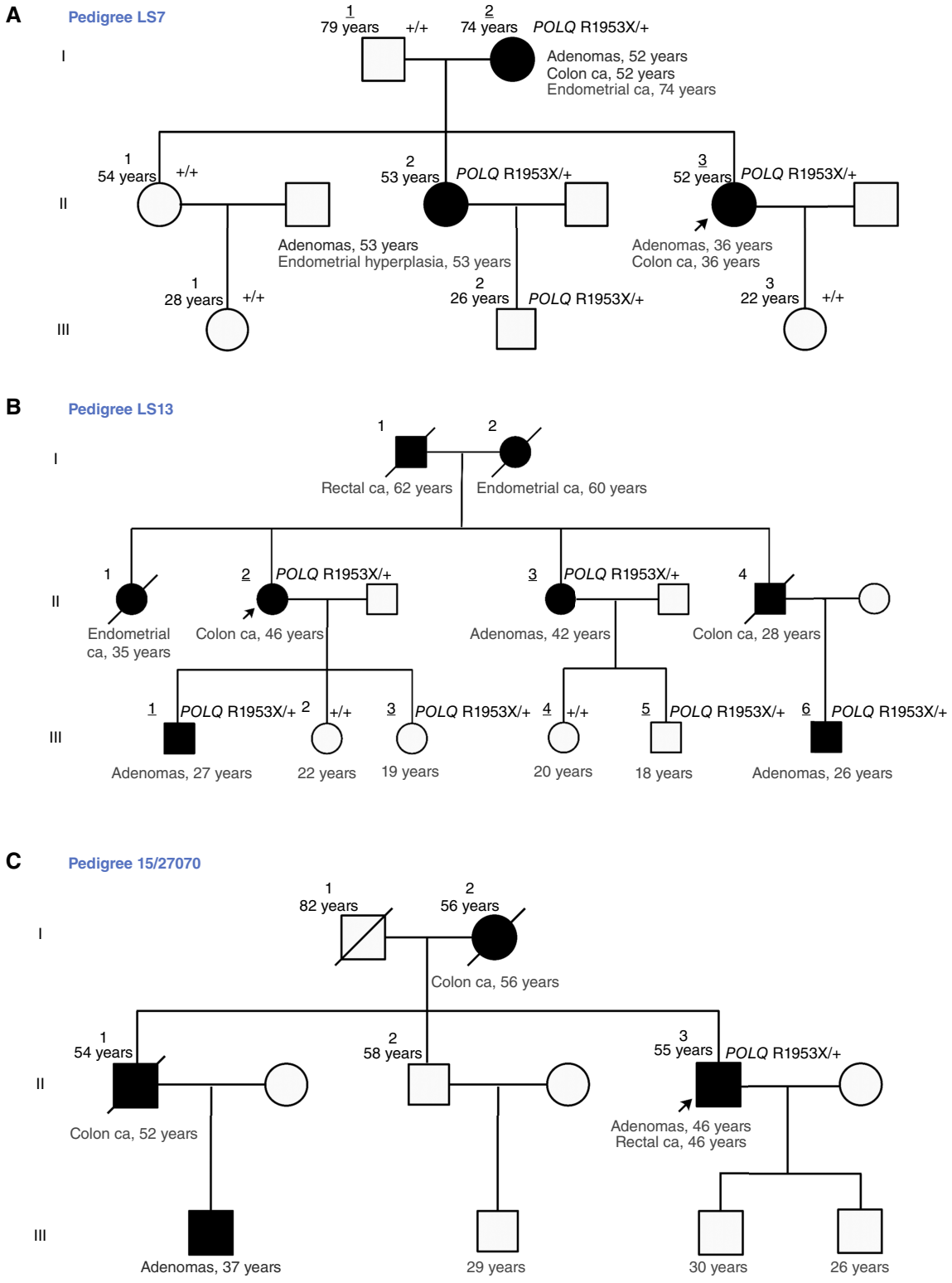

Table 1. Detection and frequency of the *POLQ* p.Arg1953X mutation in different phases and cohorts of the study.

Phase	Method	Families	Individuals	Description	Frequency (%)
Discovery	WES	12	43	12 pedigrees with hereditary CRC, 43 individuals	8.3 (1/12)
Validation	Sanger/WES	84	84	84 patients with hereditary CRC or polyposis	1.2 (1/84)
	Sanger	—	310	310 patients with sporadic CRC	0 (0/310)
	WGS	—	285	285 patients with early-onset, polyposis, and/or familial CRC	0.35 (1/285)
Total	—	97	595	3 mutated pedigrees in 97 pedigrees	3.09% (3/97)
				11 mutation carriers in 595 patients	0.50% (11/595)

This table summarizes the screening results for the *POLQ* p.Arg1953X mutation across different phases of the study.
Abbreviation: CRC, colorectal cancer.

qRT-PCR

Total RNA was isolated from cells using TRIzol reagent (Invitrogen). One microgram of total RNA was used to synthesize cDNA using M-MLV Reverse Transcriptase (Promega) in a final volume of 25 μL following the manufacturer's instructions. The relative mRNA levels of *POLQ* were quantified using qRT-PCR, normalized to β-actin. The PCR was performed in a total volume of 20 μL containing 2 μL of diluted cDNA, 10 μL of SYBR Master Mix (Bio-Rad), and 0.2 μL of each primer (10 μmol/L; Supplementary Table S1) using a Bio-Rad Real-time PCR system. Thermal cycling conditions included an initial denaturation at 95°C for 5 minutes, followed by 40 cycles of 95°C for 10 seconds and 55°C for 30 seconds.

Immunofluorescent staining of γ-H2AX

After seeding on coverslips to 60% to 70% confluency, cells were allowed to attach for 12 hours and then treated with etoposide or ultraviolet (UV). At various time points, as indicated in the corresponding figures, cells were washed with PBS and fixed in 4% paraformaldehyde for 8 minutes. After thrice washing, the cells were permeabilized with 0.2% Triton X-100. The coverslips were then blocked with 1% BSA in PBS containing 0.1% Triton X-100 and stood for 30 minutes at room temperature. The blocked coverslips were then probed with an antibody against γ-H2AX, followed by Alexa Fluor Plus 594 secondary antibody and 4′,6-diamidino-2-phenylindole (Supplementary Table S2). Images of fluorescent γ-H2AX foci was captured by confocal microscopy.

Western blotting

Cells were lysed with SDS lysis buffer (Beyotime) containing the protease inhibitor phenylmethylsulfonylfluoride and phosphatase inhibitor cocktail A. Protein concentrations were determined using a bicinchoninic acid assay kit (Beyotime). Lysates containing 50 to 80 μg of protein were separated on 8% or 12% SDS-PAGE gels and transferred to polyvinylidene difluoride membranes (Bio-Rad). Membranes were blocked with 5% skim milk for 2 hours at room temperature and then incubated with primary antibodies (Supplementary Table S2) overnight at 4°C. After washing with TBS with Tween, membranes were incubated with peroxidase-conjugated secondary antibodies (1:10,000; Seracare KPL Inc.) at 4°C overnight. The epitopes were visualized using ECL Western Blot Detection Kit (Millipore). Densitometry of each blot was evaluated using ImageJ (NIH).

Xenograft experiments

Five-week-old female BALB/c nude mice were obtained from Vital River Laboratory and kept in pathogen-free conditions. All animal procedures were approved by the Animal Ethics Committee of Kunming Medical University. Mice were fed and given water *ad libitum*. After adaptation, mice were divided into four groups ($n = 6$ per group). 293T (2×10^6) or HCT116 (1×10^6) cells were injected subcutaneously to establish xenografts. Tumor volumes and mouse weights were measured every 3 days.

For treatments, when tumors reached 60, 120, or 1,500 mm^3, mice were redivided into three groups per genotype. Treatments included IR (10 Gy), etoposide (20 mg/kg), and NVB (150 mg/kg), alone or in combination, administered via intraperitoneal injection. Etoposide and NVB were dissolved in DMSO and diluted in normal saline.

GFP reporter–based DNA repair assays

The GFP reporter–based DNA repair assays were performed as described previously (15). In brief, DR-GFP (for HR), EJ5 (for total NHEJ), and EJ2 [for θ-mediated end-joining (TMEJ)] repair substrates were purchased from Addgene (#26475, #44026, and #44025, respectively). To measure repair efficiency, 1×10^5 cells were plated in each well of a 12-well plate. Indicated compounds or DMSO were added to the medium for 24 hours, after which cells were transfected with the repair substrate and I-SceI enzyme in equal proportion. At 48 hours after transfection, cells were trypsinized, and GFP-positive cells were quantified by flow cytometry (Beckman Coulter).

Statistical analysis

All statistical analyses were performed using GraphPad Prism v10.0. Student *t* test was used for statistical analysis between two

Figure 1.

A pathogenic *POLQ* stop-gain mutation identified in hereditary colorectal cancer (CRC) pedigrees. **A,** In the discovery phase, WES was initially performed in 12 CRC pedigrees. *POLQ* p.Arg1953X mutation cosegregated with disease status in pedigree LS7, with three mutation carriers identified. **B,** *POLQ* mutation was screened using Sanger sequencing in the validation cohort, which includes 84 familial polyposis and CRC cases and 310 sporadic CRC cases. The *POLQ* p.Arg1953X mutation was found in one proband (LS13) in the validation cohort; and the family members were subsequently screened. **C,** We further screened POLQ mutation in an external expanded WGS cohort of 285 hereditary CRC patients. The *POLQ* p.Arg1953X mutation was found in one proband in the expanded validation cohort and was subsequently investigated for family information (15/27070). Clinical information suggests a link between the *POLQ* mutation and CRC or adenomas within this family. Individuals with underlined numbers underwent WES; "ca." denotes cancer, with numbers indicating age at diagnosis.

groups. All tests were two-tailed. All data are represented as the mean ± SD. A *P*-value of <0.05 was considered statistically significant.

Data availability

Data generated or analyzed during this study are included in this article and its Supplementary Materials. Raw sequencing data of

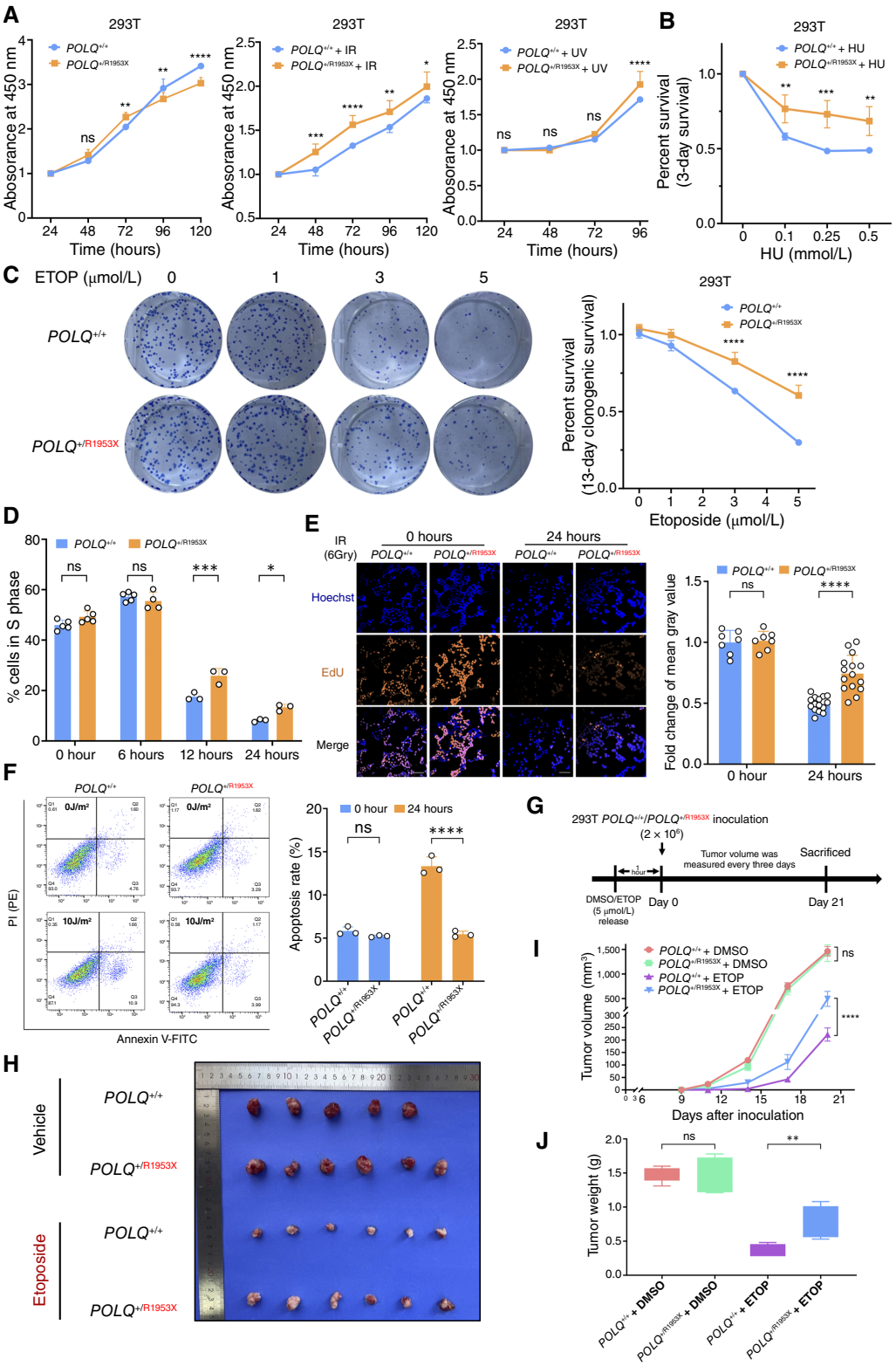

human subjects are available from the authors upon reasonable request due to privacy/ethical restrictions. WGS results of $POLQ^{+/R1953X}$ HCT116 cells are accessible, in the format of VCF files, at http://mitotool.kiz.ac.cn/lab/download/HCT116_WT_POLQ_WGS.tar. The WGS raw data have been deposited in the National Genomics Data Center with accession ID HRA011160 (publicly accessible at https://ngdc.cncb.ac.cn/gsa-human/browse/HRA011160).

Results

Identifying *POLQ* as a new pathogenic gene for hereditary colorectal cancer

WES was performed on 43 individuals from 12 families with hereditary colorectal cancer, each including at least two affected individuals and one healthy control (**Fig. 1A**; Supplementary Fig. S1A). In family LS6, an *MSH2* variant (p.Arg645*), known for its association with MMR deficiency, was identified (Supplementary Table S3). Further analysis led to the discovery of a novel germline mutation in the *POLQ* gene (c.5857C>T, p.Arg1953X) in family LS7, confirmed by Sanger sequencing (**Fig. 1A**; Supplementary Table S4). The mutation has a high CADD (Combined Annotation Dependent Depletion, https://cadd.gs.washington.edu/) score of 42, indicating potential pathogenicity. Although previously reported as a somatic mutation in colorectal cancer organoids and astrocytic tumors, no link to hereditary colorectal cancer had been established (16, 17).

The *POLQ* p.Arg1953X variant was found in 34 individuals worldwide in the gnomAD database, with a higher frequency (0.03%) among East Asians. During the validation phase, 84 probands from families with polyposis and 310 sporadic colorectal cancer cases were screened (**Table 1** and; Supplementary Table S5). As shown in **Table 1**, the *POLQ* p.Arg1953X mutation was found in 1.2% (1/84) of the families with polyposis and was absent in the sporadic cases. This validation cohort identified one additional family (LS13) with the same mutation (**Fig. 1B**). In both LS7 and LS13 families, 70% of mutation carriers had adenomatous polyps or colorectal cancer, whereas all WT individuals were unaffected, suggesting a strong genotype–phenotype correlation (Supplementary Table S6).

Both LS7 and LS13 families exhibited adenomatous polyposis and a high risk of colorectal cancer, with adenoma counts ranging from 10 to 22 in LS7 and 8 to 17 in LS13 (Supplementary Table S7). Genetic testing for other relevant genes (e.g., *POLE*, *POLD1*, and *MMR*) revealed no pathogenic variants, and IHC confirmed normal MMR protein expression, further supporting *POLQ* p.Arg1953X as a novel driver of adenomatous polyposis in these families (Supplementary Fig. S1B).

The p.Arg1953X mutation showed dominant inheritance with high penetrance for adenomas and carcinomas. Among the 10 carriers, six had colorectal adenomas or carcinomas, and two developed extracolonic conditions: one developed endometrial cancer (LS7-I-2), and another developed endometrial complex hyperplasia (LS7-II-2), which may indicate a predisposition to endometrial cancer (Supplementary Table S7). The independent occurrence of the mutation in LS7 and LS13, along with the absence of other known pathogenic variants, reinforces *POLQ* p.Arg1953X as a novel hereditary colorectal cancer mutation.

Additionally, in the expanded WGS cohort of 285 individuals with potential hereditary colorectal cancer (early-onset, multiple polyps, and/or family history), one individual carrying a heterozygous *POLQ* p.Arg1953X mutation was identified (in pedigree 15/27070). This individual was diagnosed with rectal cancer at age 46 and had multiple colonic adenomas. Family history indicated a potential link to colorectal cancer and adenomas, and this individual can be considered belonging to a *POLQ* p.Arg1953X–positive family. This finding hints at the relevance of this mutation (**Fig. 1C**). The mutation was absent in sporadic cases in the study validation phase (**Table 1**).

Isogenic cell lines with *POLQ* p.Arg1953X mutation exhibit higher viability in response to DNA damage

To investigate the role of the *POLQ* p.Arg1953X mutation in tumor development, we used CRISPR/Cas9-mediated HR to introduce this mutation into 293T and HCT116 cell lines, creating $POLQ^{+/R1953X}$ and $POLQ^{R1953X/R1953X}$ variants, alongside a *POLQ* KO ($POLQ^{-/-}$) HCT116 line for comparison (Supplementary Fig. S2). *POLQ* is critical for repairing DNA double-strand breaks (18, 19). We found that $POLQ^{+/R1953X}$ cells had reduced viability under normal conditions but showed enhanced resistance to IR and UV exposure, indicating a greater resilience to DNA damage (**Fig. 2A**). Survival assays demonstrated that increasing concentrations of hydroxyurea, etoposide reduced cell survival in a dose-dependent manner, but $POLQ^{+/R1953X}$ cells were less affected compared with WT (**Fig. 2B** and **C**). The p.Arg1953X mutation facilitated accelerated cell-cycle progression after DNA damage, notably increasing DNA synthesis during the S phase, as confirmed by the EdU incorporation assay (**Fig. 2D** and **E**). This mutation also conferred resistance to apoptosis (**Fig. 2F**). *In vivo* experiments with nude mice inoculated with $POLQ^{+/+}$ and $POLQ^{+/R1953X}$ cells pretreated with DNA-damaging agents revealed that the heterozygous mutation promoted xenograft growth, increasing both tumor volume and weight (**Fig. 2G–J**). These findings suggest that the $POLQ^{+/R1953X}$ mutation enhances resistance to DNA damage, thereby promoting tumorigenesis.

Heterozygous p.Arg1953X mutation leads to overactivation of WT *POLQ* allele under DNA damage stress

The p.Arg1953X mutation introduces a premature termination codon (PTC), which was initially thought to cause protein

Figure 2.

POLQ p.Arg1953X mutation promotes cell survival and apoptosis resistance under DNA damage stress. **A,** Viability of cells with heterozygous *POLQ* p.Arg1953X mutation ($POLQ^{+/R1953X}$) under UV (10 J/m^2) or IR (4 Gy) in a CCK-8 assay. **B** and **C,** Enhanced survival of $POLQ^{+/R1953X}$ cells compared with $POLQ^{+/+}$ cells under hydroxycarbamide (HU, 0–0.5 mmol/L) and etoposide (0–5 μmol/L) treatment. **D,** Accumulation of $POLQ^{+/R1953X}$ cells in the S phase under IR (6 Gy) as shown by flow cytometry. **E,** EdU incorporation to indicate cell-cycle fractions of 293T cells at 0 and 24 hours after IR. Images taken at 100× magnification. **F,** Resistance of $POLQ^{+/R1953X}$ cells to UV-induced apoptosis (10 J/m^2) detected via annexin V/PI staining after 24 hours. **G–J,** Tumor growth promotion by the *POLQ* p.Arg1953X mutation in xenograft models under DNA-damaging conditions. **G,** Xenografting protocol for DNA-damaged 293T cells into BALB/c nude mice. **H,** *In vivo* tumor growth promotion by $POLQ^{+/R1953X}$ cells treated with etoposide or DMSO. **I** and **J,** Tumor volumes and weights measured on day 21 after inoculation. All phenotypic experiments in this figure were performed using 293T cells. Data are shown as the mean ± SD. Student *t* test was used for statistical analysis. *, $P < 0.05$; **, $P < 0.01$; ***, $P < 0.001$; ****, $P < 0.0001$. ETOP, etoposide; ns, not significant.

haploinsufficiency or truncated peptides (20, 21). Indeed, we found lower total *POLQ* mRNA levels in individuals with the p.Arg1953X mutation compared with noncarriers (**Fig. 3A**). Similarly, *POLQ*$^{+/R1953X}$ 293T and HCT116 cells had reduced *POLQ* mRNA compared with *POLQ*$^{+/+}$ cells (**Fig. 3B**). To confirm that this reduction was due to nonsense-mediated mRNA decay (NMD), we

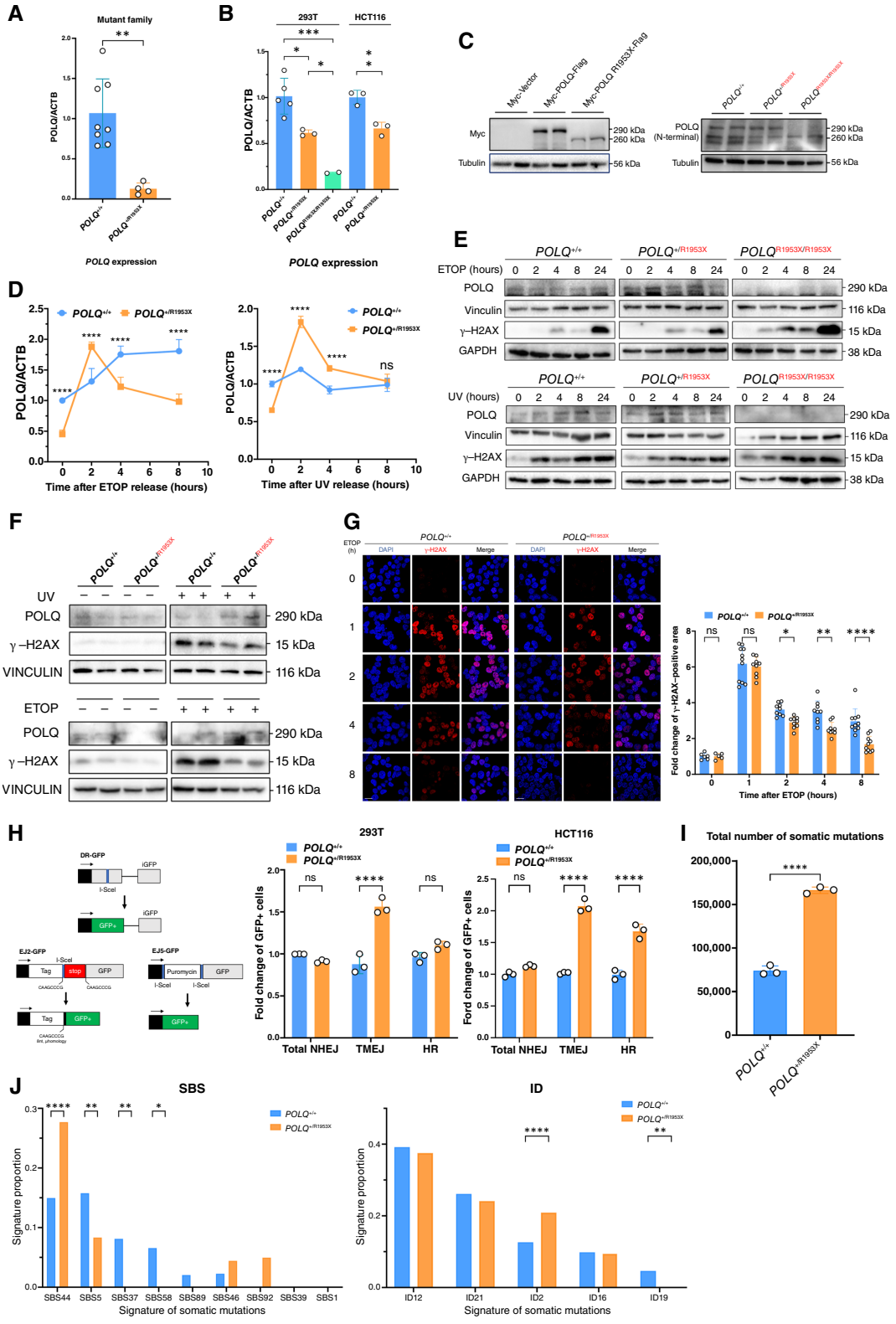

knocked down UPF1, a key NMD factor (22). *UPF1* knockdown restored *POLQ* mRNA expression (Supplementary Fig. S3), indicating that the p.Arg1953X mutation triggers NMD. However, Western blotting with an N-terminal *POLQ* antibody revealed similar protein levels between $POLQ^{+/R1953X}$ and $POLQ^{+/+}$ cells, with *POLQ* protein undetectable in $POLQ^{R1953X/R1953X}$ cells, indicating no truncated allele formation and compensated expression of WT allele (**Fig. 3C**).

Despite the initial reduction in *POLQ* mRNA levels due to NMD, $POLQ^{+/R1953X}$ cells exhibit a significant increase in *POLQ* expression following DNA damage. Two hours after exposure to DNA-damaging agents, qPCR and Western blotting analysis of 293T cells revealed an upregulation of *POLQ* expression specifically from the WT allele in $POLQ^{+/R1953X}$ cells following treatment with UV light or etoposide (**Fig. 3D** and **E**). This suggests that whereas the p.Arg1953X mutation initially leads to NMD, it triggers a compensatory mechanism under DNA damage stress, enhancing the expression of the WT *POLQ* allele to maintain sufficient protein levels for DNA repair. This response indicates that the p.Arg1953X mutation activates an adaptive molecular response that supports cellular survival and potentially contributes to tumorigenesis by enhancing DNA repair capabilities under stress conditions (23).

POLQ p.Arg1953X mutation promotes DNA repair via the TMEJ pathway

To evaluate the functional impact of the *POLQ* p.Arg1953X mutation on DNA repair, we first examined the cellular response to etoposide- and UV-induced DNA damage. Compared with $POLQ^{+/+}$ 293T cells, $POLQ^{+/R1953X}$ cells exhibited markedly reduced γ-H2AX levels, as shown by both Western blotting and immunofluorescence (**Fig. 3F** and **G**), indicating enhanced DNA repair efficiency. Notably, *POLQ* protein levels were significantly higher in $POLQ^{+/R1953X}$ cells than in $POLQ^{+/+}$ cells under DNA-damaging conditions, as detected using N-terminal antibodies (**Fig. 3F**), suggesting that stress-induced overexpression of the WT *POLQ* allele may contribute to this phenotype.

To directly assess the activity of different DNA repair pathways, we used GFP-based reporter assays to quantify total NHEJ, TMEJ, and HR (24). $POLQ^{+/R1953X}$ cells demonstrated increased total NHEJ and TMEJ activity relative to $POLQ^{+/+}$ cells (**Fig. 3H**), indicating that the p.Arg1953X mutation promotes end-joining repair through upregulation of *POLQ* expression.

To explore the genomic consequences of this enhanced repair activity, we performed WGS of $POLQ^{+/+}$ and $POLQ^{+/R1953X}$ HCT116 cells. $POLQ^{+/R1953X}$ cells displayed a significantly higher overall mutation burden (**Fig. 3I**), suggesting genome-wide accumulation of DNA alterations. Mutational signature analysis revealed elevated contributions of specific single-base substitution (SBS) signatures—particularly SBS44, SBS5, SBS37, and SBS58—as well as an increased indel burden primarily driven by ID2 (**Fig. 3J**). Together, these findings demonstrate that although the p.Arg1953X mutation enhances TMEJ-mediated repair, it also induces distinct mutational consequences across the genome.

Higher somatic mutation burden in tumor from *POLQ* p.Arg1953X carriers

The error-prone nature of TMEJ-mediated DNA repair suggests that $POLQ^{+/R1953X}$ carriers may exhibit a higher somatic mutation burden (25, 26). We sequenced 769 cancer-related genes in colorectal cancer tumors from two *POLQ* mutation carriers (LS7 I:2 and LS13 II:2) and compared them with 320 individuals without the mutation. The carriers displayed high TMB at 80.85 and 65.26 mutations per Mb, respectively, which is characteristic of hypermutated colorectal cancers (**Fig. 4A** and **B**; ref. 27). Additionally, both tumors were classified as MSI-H based on the sequencing analysis.

The tumors contained 89 and 80 nonsynonymous mutations, with alterations in key DNA repair genes such as *MSH2*, *ATM*, *POLE*, *POLD1*, *MUTYH*, *BRCA2*, and *TP53* (Supplementary Table S8). High mutation frequencies were also observed in genes like *KMT2D*, *PTPRS*, and *CREBBP*, as well as regions on chromosomes 12, 16, and 6, suggesting potential oncogenes or regulatory elements (**Fig. 4C–E**; Supplementary Fig. S4; refs. 27–29). The somatic mutations likely drive tumorigenesis, mimicking MMR deficiency, as indicated by a predominant C>T mutation pattern (**Fig. 4F**; ref. 30). Signature analysis showed elevated levels of SBS1, SBS3, SBS5, and SBS13, associated with background mutations, HR defects, and APOBEC activity (**Fig. 4G**; Supplementary Table S9; refs. 31–34). Additionally, ID signature analysis revealed high frequencies of ID13 and ID23, which are linked to MSI, further indicating genomic instability (**Fig. 4H**; Supplementary Table S9; refs. 31, 35). Notably, the signature of tumors is not exactly the same with the above mutated HCT116 cells, indicating the complexity of *POLQ*-related DNA repair signature.

MSI analysis confirmed the MSI-H status of the carriers (**Fig. 4I**), revealing significant allele shifts (36), whereas loss of heterozygosity analysis suggested that gene amplification, rather than loss of heterozygosity, might be contributing to allelic imbalances in these tumors (37, 38). These findings provide direct evidence connecting the *POLQ* p.Arg1953X mutation to a high somatic mutation burden and MSI-H status in hereditary colorectal cancer, with gene amplification potentially driving tumorigenesis.

Figure 3.

POLQ p.Arg1953X may drive tumorigenesis through error-prone TMEJ DNA repair pathway. **A,** Decreased *POLQ* mRNA expression in blood samples from p.Arg1953X carriers, indicating NMD. The house-keeping gene *ACTB* (Actin Beta) was used for normalization. **B,** Lower *POLQ* mRNA levels in $POLQ^{+/R1953X}$ cells (293T and HCT116 cells) compared with $POLQ^{+/+}$ cells, consistent with blood sample data. **C,** Western blot shows comparable *POLQ* protein levels in $POLQ^{+/R1953X}$ and $POLQ^{+/+}$ 293T cells, with no truncated protein in $POLQ^{R1953X/R1953X}$ cells. **D** and **E,** Elevated *POLQ* expression upon DNA damage stress in $POLQ^{+/R1953X}$ 293T cells. **F,** Increased *POLQ* protein levels and reduced DNA damage in $POLQ^{+/R1953X}$ 293T cells treated with UV or etoposide. **G,** Reduced DNA double-strand breaks in $POLQ^{+/R1953X}$ 293T cells treated with etoposide, as shown by γ-H2AX levels. Scale bars, 20 μm. Data are shown as the mean ± SD. **H,** Enhanced TMEJ activity in 293T cells carrying the p.Arg1953X mutation, as shown by reporter assay. **I,** WGS shows a significantly higher total mutation burden in $POLQ^{+/R1953X}$ HCT116 cells compared with $POLQ^{+/+}$ cells, indicating genome-wide accumulation of mutations associated with the p.Arg1953X variant. **J,** Mutational signature analysis based on WGS data. Left: $POLQ^{+/R1953X}$ cells exhibit increased burden of SBS signatures, notably SBS44, suggesting enhanced mismatch-related substitutions. Right: ID signature analysis reveals a significant enrichment of ID12 and ID19 in $POLQ^{+/R1953X}$ cells, consistent with altered small indel repair activity. Statistical significance: *, $P < 0.05$; **, $P < 0.01$; ***, $P < 0.001$; ****, $P < 0.0001$; ns, not significant. DAPI, 4′,6-diamidino-2-phenylindole; ETOP, etoposide.

Introduction of another PTC, POLQ p.Gln1949X, mimics Arg1953X-related phenotypes

To verify the PTC-mediated mechanism, we introduced an artificial heterozygous PTC mutation, p.Gln1949X, into the 293T and HCT116 cell lines ($POLQ^{+/Q1949X}$ and $POLQ^{Q1949X/Q1949X}$). Control lines with a Q1949X PTC also showed reduced mRNA and no truncated peptide (Supplementary Fig. S5A and S5B). Similarly, tumor-prone resistance of DNA damage was observed in the

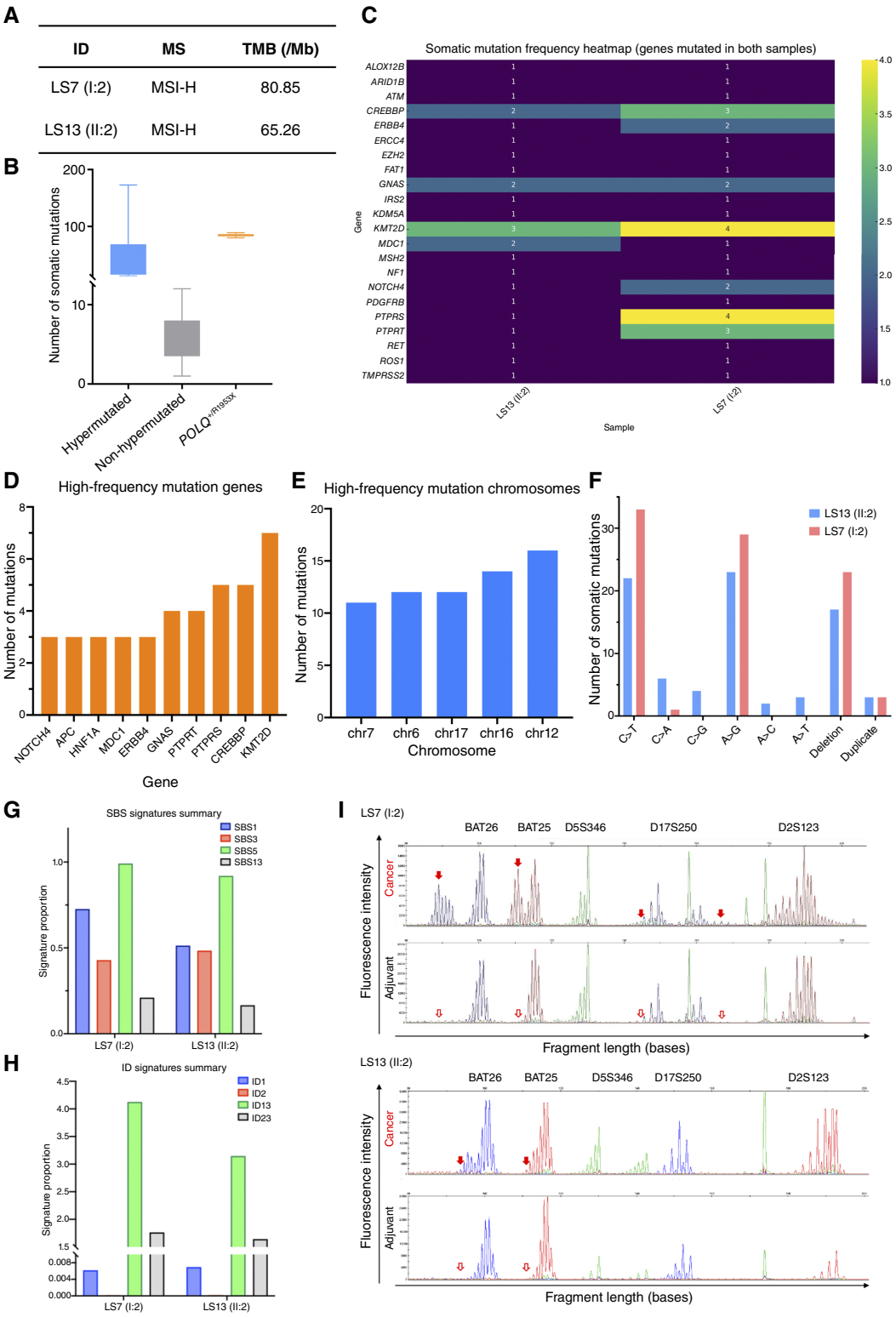

survival assays of the $POLQ^{+/Q1949X}$ 293T and HCT116 cells. Both the 293T and HCT116 cell lines with p.Gln1949X exhibited better survival under DNA damage stress induced by IR and etoposide (Supplementary Fig. S5C and S5D). The $POLQ^{+/Q1949X}$ HCT116 cells showed increased *POLQ* protein and decreased γ-H2AX levels under UV treatment (Supplementary Fig. S5E–S5G), mediated by enhanced TMEJ activity (Supplementary Fig. S5H). These results indicate that PTC mutations lead to compensated overexpression of the WT allele of *POLQ* under DNA damage, which, in turn, causes overactivation of the TMEJ pathway, resulting in enhanced error-prone DNA repair.

POLQ KO cells exhibit distinct phenotypes under DNA damage

To further confirm whether the Arg1953X mutation is gain-of-function or similar to loss-of-function, we generated *POLQ* KO ($POLQ^{-/-}$) HCT116 cells and assessed their proliferation, survival, apoptosis, DNA repair efficiency, and tumor growth under IR treatment. CCK-8 assays demonstrated that $POLQ^{-/-}$ cells exhibited significantly reduced proliferation rates under IR treatment compared with $POLQ^{+/+}$ and $POLQ^{+/R1953X}$ cells (Supplementary Fig. S6A). Clonogenic assays further confirmed the decreased survival of $POLQ^{-/-}$ cells, as indicated by their reduced ability to form colonies under IR treatment (Supplementary Fig. S6B). Annexin V/PI staining showed that $POLQ^{-/-}$ cells had a higher apoptosis rate compared with $POLQ^{+/+}$ and $POLQ^{+/R1953X}$ cells after IR treatment (Supplementary Fig. S6C). To assess the impact of *POLQ* KO on tumor growth, we performed *in vivo* xenograft experiments. $POLQ^{-/-}$ HCT116 cells exhibited significantly reduced tumor growth in nude mice compared with $POLQ^{+/+}$ and $POLQ^{+/R1953X}$ cells (Supplementary Fig. S6D–S6G). Furthermore, GFP reporter assays (Supplementary Fig. S6H) indicated that TMEJ repair activity was significantly reduced in $POLQ^{-/-}$ HCT116 cells, whereas HR activity was significantly increased compared with $POLQ^{+/+}$ and $POLQ^{+/R1953X}$ cells, highlighting a notable difference in DNA repair pathway utilization.

These findings indicate that the loss of *POLQ* significantly impairs DNA repair and cell survival, leading to increased apoptosis and reduced tumor growth, in contrast to the activation of DNA repair pathways observed in $POLQ^{+/R1953X}$ cells, adding more support that the Arg1953X mutation contributes to tumorigenesis in a gain-of-function manner rather than loss-of-function (or haploinsufficiency).

Targeting the TMEJ pathway reverses *POLQ* PTC mutation–associated tumorigenesis-relevant phenotypes

POLQ-PTC mutation carriers exhibit increased resistance to DNA damage, posing a treatment challenge. Etoposide effectively inhibited $POLQ^{+/+}$ cell growth, but $POLQ^{+/R1953X}$ cells were resistant (**Fig. 2H–K**). We hypothesized that inhibiting the TMEJ pathway with NVB, an FDA-approved *POLQ* inhibitor (39), might counteract this resistance. Reporter assays confirmed that NVB suppressed TMEJ activity across *POLQ* genotypes (**Fig. 5A**). Notably, total NHEJ and HR activities increased in $POLQ^{+/+}$, but not $POLQ^{+/R1953X}$, cells after NVB treatment, suggesting that NVB can reverse the tumorigenic phenotype of *POLQ* MUT cells. This was supported by increased γ-H2AX expression after UV treatment in NVB-treated $POLQ^{+/R1953X}$ 293T cells (**Fig. 5B** and **C**).

We tested whether NVB could reduce DNA damage resistance in $POLQ^{+/R1953X}$ cells. Under DNA damage stress, NVB significantly reversed UV-induced resistance in $POLQ^{+/R1953X}$ cells compared with $POLQ^{+/+}$ cells (**Fig. 5D**). In 293T xenograft experiments, NVB enhanced the inhibitory effect of etoposide on $POLQ^{+/R1953X}$ xenografts, reducing tumor growth (**Fig. 5E–H**). NVB also increased radiosensitivity in $POLQ^{+/R1953X}$ HCT116 xenografts, improving response to radiotherapy (Supplementary Fig. S7A–S7D).

These results demonstrate that NVB counteracts DNA damage resistance in *POLQ* mutation carriers by targeting the TMEJ pathway, underscoring the role of TMEJ overactivation in DNA repair enhancement in cells with *POLQ* heterozygous PTC mutations.

Discussion

This study identifies *POLQ* as a novel pathogenic gene in hereditary colorectal adenomatous polyposis, linked to a germline heterozygous stop-gain mutation, p.Arg1953X. This mutation predisposes individuals to early-onset colorectal cancer and multiple adenomas, defining a *POLQ*-associated cancer syndrome. The syndrome presents a multiple-adenoma phenotype similar to *MUTYH*-associated polyposis (3). Our findings suggest that *POLQ* mutation, a novel driver in hereditary adenomatous polyposis, contributes to a substantial proportion of previously undefined hereditary colorectal cancer cases and highlights the need to screen for *POLQ* mutations in patients with multiple adenomas. Nevertheless, further research with larger cohorts is needed to determine whether there is a statistically significant relationship between *POLQ* mutations and extracolonic malignancies.

Carriers of the *POLQ* p.Arg1953X mutation develop multiple adenomas (8–22 per patient) and colorectal cancer at an early age, with onset as early as 36 years. Given the evidence of frequent *POLQ* stop-gain mutations in databases like gnomAD, genetic testing for *POLQ* mutations, particularly in patients with multiple adenomas or early-onset colorectal cancer, is warranted (40). Our findings expand the understanding of hereditary colorectal cancer and suggest *POLQ*'s critical role in adenomatous polyposis predisposition.

Mechanistically, the heterozygous p.Arg1953X mutation does not lead to haploinsufficiency or truncated protein but instead triggers NMD and upregulation of the WT *POLQ* allele in response to DNA damage (20, 41). This is further supported by the distinct phenotype observed in *POLQ* KO cells, which exhibit decreased DNA repair function, indicating the essential role of WT *POLQ* in maintaining DNA repair capacity. Together with the fact that the gain-of-function phenotypes in the heterozygous mutation cells were reversed by *POLQ* inhibition, it is evident that the nonsense mutation leads to the activation or gain-of-function of *POLQ* protein. This compensatory

Figure 4.

High somatic mutation burden in tumors from *POLQ* p.Arg1953X carriers. **A,** Elevated TMB and MSI-H in carriers within LS7 (I:2) and LS13 (II:2), with TMB values of 80.85 and 65.26 mutations/Mb. **B,** The number of nonsynonymous mutations in these tumors falls within the hypermutated colorectal cancer range. **C,** Tumors from *POLQ* p.Arg1953X carriers in LS7 and LS13 share somatic mutations in oncogenes like ATM and MSH2. **D,** High mutation frequencies observed in genes such as *KMT2D*, *PTPRS*, and *CREBBP* in both probands, with the total number of mutations summed. **E,** Chromosomes (chr) 12, 16, and 6 exhibit high mutation frequencies, suggesting possible oncogenic or regulatory elements. **F,** Mutation patterns reveal a bias toward C>T transitions and indels, typical of MMR-deficient cancers. **G** and **H,** SBS and ID signature analyses reveal elevated SBS1, SBS3, SBS5, SBS13, and high ID13 and ID23 frequencies, indicative of DNA repair deficiencies. **I,** MSI analysis confirms MSI-H in both LS7 and LS13 using the Bethesda panel. LOH analysis suggests gene amplification over loss of heterozygosity (LOH).

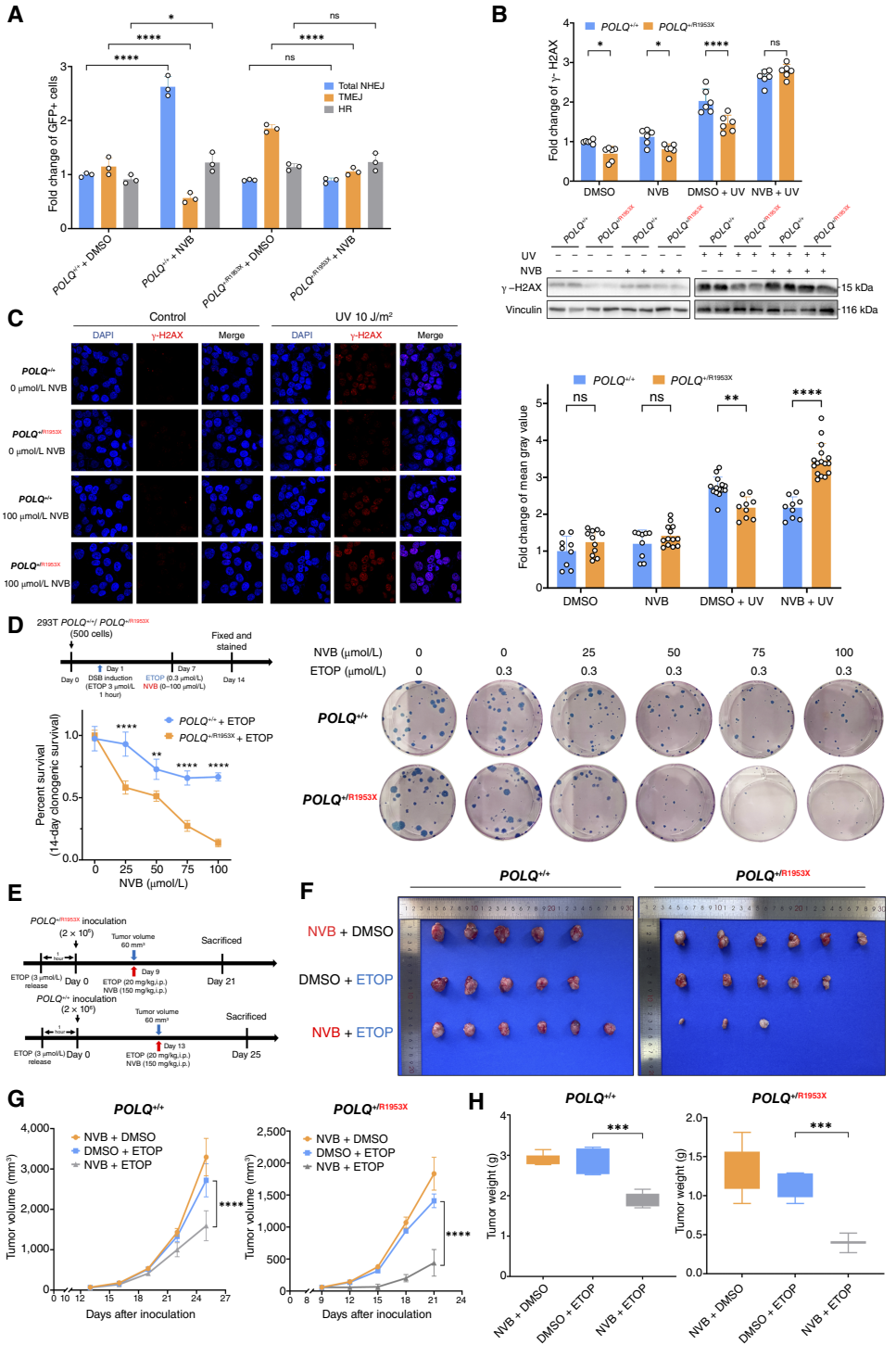

Figure 5.

NVB modulates the TMEJ pathway to reverse *POLQ*-p.Arg1953X phenotypes. **A,** NVB (100 μmol/L), a *POLQ* inhibitor, reduces TMEJ activity in $POLQ^{+/R1953X}$ cells compared with $POLQ^{+/+}$ cells. **B** and **C,** NVB reverses UV-induced DNA damage resistance in $POLQ^{+/R1953X}$ cells, as shown by γ-H2AX expression in Western blot and immunofluorescence. Scale bars, 20 μm. **D,** Colony formation assays show that NVB reverses the abnormal proliferation of $POLQ^{+/R1953X}$ cells under DNA damage stress. **E–H,** *In vivo* inhibition of $POLQ^{+/R1953X}$ xenograft growth with NVB after DNA damage. **E,** Experimental schematic of DNA-damaged 293T cells treated with etoposide and NVB, xenografted into BALB/c mice. **F,** Images of xenograft. Statistical analysis of tumor volumes (**G**) and tumor weights (**H**) in different groups ($n = 6$/group). WT and $POLQ^{+/R1953X}$ 293T cells were used for all cellular and xenograft assays. Statistical significance: *, $P < 0.05$; **, $P < 0.01$; ***, $P < 0.001$; ****, $P < 0.0001$; ns, not significant. Data are presented as the mean ± SD. DAPI, 4′,6-diamidino-2-phenylindole; DSB, double-strand break; ETOP, etoposide.

mechanism enhances the TMEJ DNA repair pathway, contributing to tumor cell survival under stress, including resistance to chemotherapy and radiotherapy. Furthermore, *POLQ* MUT tumors exhibit a hypermutated, MSI-H phenotype, with secondary mutations in key tumor-suppressor and DNA repair genes like *MSH2*, *POLE*, and *TP53*, driving tumor progression (Supplementary Table S8; refs. 42, 43). Although HCT116 colorectal cancer cells would better recapitulate the *POLQ* function in colorectal cancer development, we observed similar results in 293T cells, suggesting that *POLQ* R1953X mutation drives tumorigenesis. This compensatory mechanism of *POLQ* upregulation highlights a previously uncharacterized adaptive response under DNA damage stress. Notably, future studies are

needed to investigate the specific molecular events responsible for this phenomenon and to confirm whether there are any functional effects of the truncated protein.

Therapeutically, targeting the TMEJ pathway with the *POLQ* inhibitor NVB reversed DNA damage resistance in *POLQ* MUT cells and enhanced the effects of radiotherapy in xenograft models. These findings highlight NVB's potential as a treatment for *POLQ* mutation carriers. However, the exact role of TMEJ in MSI-H and MMR-proficient tumors requires further exploration.

WGS revealed a significant increase in overall mutation burden in $POLQ^{+/R1953X}$ cells compared with $POLQ^{+/+}$ cells, indicating that the p.Arg1953X mutation, while enhancing repair activity, is associated with elevated genomic instability. Mutational signature analysis further showed enrichment of SBS44, SBS5, SBS37, SBS58, and the indel signature ID2, suggesting that *POLQ* activation promotes a distinct mutational landscape beyond classical TMEJ profiles. These findings underscore the tumor-promoting role of *POLQ* mutation through altered DNA repair activity.

Despite robust clinical and functional validations, this study has certain limitations. First, most cellular experiments were conducted in 293T and HCT116 cell lines; future studies should validate our findings in a wider range of colorectal cancer cell lines. Second, whereas hydroxyurea and etoposide are useful for studying DNA repair, they are not first-line colorectal cancer drugs, limiting the clinical relevance of our *in vitro* results. Future studies should utilize more clinically relevant compounds. Third, more investigation is needed to elucidate the precise mechanism by which the *POLQ* p.Arg1953X mutation leads to TMEJ hyperactivity and WT allele upregulation. Furthermore, whereas the cosegregation pattern of the *POLQ* mutation with colorectal cancer is evident in different pedigrees, we cannot definitively rule out the possibility of other genetic cause in the analyzed pedigrees; for instance, there might be regulatory variants affecting expression or function of *MLH1* or other MMR genes. In addition, our study is limited by the lack of comprehensive structural variation analysis in MMR genes like *MSH2* and *EPCAM*. Finally, clinical trials are essential to validate the therapeutic potential of NVB. Future research should focus on validating the tumorigenic role of *POLQ* mutations *in vivo* and refining therapeutic strategies targeting TMEJ.

In summary, we define a *POLQ*-associated hereditary colorectal cancer syndrome driven by the p.Arg1953X mutation. This mutation enhances the TMEJ DNA repair pathway, leading to genomic instability and treatment resistance, making *POLQ* a promising therapeutic target. Patients with multiple adenomas or early-onset colorectal cancer should be screened for *POLQ* mutations to facilitate early diagnosis and targeted therapy.

Authors' Disclosures

No disclosures were reported.

Authors' Contributions

N. Xu: Conceptualization, data curation, software, formal analysis, validation, investigation, visualization, writing–original draft. **D.-F. Zhang:** Conceptualization, software, formal analysis, funding acquisition, validation, project administration, writing–review and editing. **X.-X. Shi:** Data curation. **K.-X. Yang:** Data curation, formal analysis. **B.-B. Gan:** Investigation, methodology. **Y. Fan:** Investigation. **F.-C. Huang:** Data curation. **J.-Y. Ren:** Data curation. **R. Bi:** Writing–original draft. **Y. Li:** Methodology. **M.-S. Ye:** Investigation, methodology. **M. Xu:** Software, investigation. **Y.-C. Zhou:** Data curation, software, investigation. **W.-H. Li:** Data curation. **Y.-G. Yao:** Conceptualization, data curation, writing–review and editing. **W.-L. Li:** Conceptualization, resources, supervision, funding acquisition, validation, methodology, writing–review and editing.

Acknowledgments

This study was supported by the National Natural Science Foundation of China (grants 31660312 and 82160563) and Yunnan Province (grants 202403AC100001, 202501AT070132, and 202305AH340006). We gratefully acknowledge those patients who volunteered to participate in the study and agreed to provide research biopsies. We thank the staff members of the National Research Facility for Phenotypic & Genetic Analysis of Model Animals (Primate Facility) (https://cstr.cn/31137.02.NPRC), for providing technical support and assistance in data collection and analysis.

Note

Supplementary data for this article are available at Clinical Cancer Research Online (http://clincancerres.aacrjournals.org/).

Received January 30, 2025; revised April 17, 2025; accepted May 21, 2025; posted first May 27, 2025.

References

1. Jasperson KW, Tuohy TM, Neklason DW, Burt RW. Hereditary and familial colon cancer. Gastroenterology 2010;138:2044–58.
2. Boland PM, Yurgelun MB, Boland CR. Recent progress in Lynch syndrome and other familial colorectal cancer syndromes. CA Cancer J Clin 2018;68:217–31.
3. Aelvoet AS, Buttitta F, Ricciardiello L, Dekker E. Management of familial adenomatous polyposis and MUTYH-associated polyposis; new insights. Best Pract Res Clin Gastroenterol 2022;58–59:101793.
4. Giardiello FM, Brensinger JD, Petersen GM, Luce MC, Hylind LM, Bacon JA, et al. The use and interpretation of commercial APC gene testing for familial adenomatous polyposis. N Engl J Med 1997;336:823–7.
5. Valle L, Vilar E, Tavtigian SV, Stoffel EM. Genetic predisposition to colorectal cancer: syndromes, genes, classification of genetic variants and implications for precision medicine. J Pathol 2019;247:574–88.
6. Weren RDA, Ligtenberg MJL, Kets CM, de Voer RM, Verwiel ETP, Spruijt L, et al. A germline homozygous mutation in the base-excision repair gene NTHL1 causes adenomatous polyposis and colorectal cancer. Nat Genet 2015;47:668–71.
7. Palles C, Cazier J-B, Howarth KM, Domingo E, Jones AM, Broderick P, et al. Germline mutations affecting the proofreading domains of POLE and POLD1 predispose to colorectal adenomas and carcinomas. Nat Genet 2013;45:136–44.
8. Jeggo PA, Pearl LH, Carr AM. DNA repair, genome stability and cancer: a historical perspective. Nat Rev Cancer 2016;16:35–42.
9. Li H, Durbin R. Fast and accurate short read alignment with Burrows-Wheeler transform. Bioinformatics 2009;25:1754–60.
10. Tate JG, Bamford S, Jubb HC, Sondka Z, Beare DM, Bindal N, et al. COSMIC: the catalogue of somatic mutations in cancer. Nucleic Acids Res 2019;47:D941–7.
11. Danecek P, Bonfield JK, Liddle J, Marshall J, Ohan V, Pollard MO, et al. Twelve years of SAMtools and BCFtools. Gigascience 2021;10:giab008.
12. Khandekar A, Vangara R, Barnes M, Díaz-Gay M, Abbasi A, Bergstrom EN, et al. Visualizing and exploring patterns of large mutational events with SigProfilerMatrixGenerator. BMC Genomics 2023;24:469.
13. Rosenthal R, McGranahan N, Herrero J, Taylor BS, Swanton C. DeconstructSigs: delineating mutational processes in single tumors distinguishes DNA repair deficiencies and patterns of carcinoma evolution. Genome Biol 2016;17:31.
14. Bi R, Li Y, Xu M, Zheng Q, Zhang D-F, Li X, et al. Direct evidence of CRISPR-Cas9-mediated mitochondrial genome editing. Innovation (Camb) 2022;3:100329.
15. Bennardo N, Cheng A, Huang N, Stark JM. Alternative-NHEJ is a mechanistically distinct pathway of mammalian chromosome break repair. PLoS Genet 2008;4:e1000110.

16. van de Wetering M, Francies HE, Francis JM, Bounova G, Iorio F, Pronk A, et al. Prospective derivation of a living organoid biobank of colorectal cancer patients. Cell 2015;161:933–45.
17. Killela PJ, Pirozzi CJ, Reitman ZJ, Jones S, Rasheed BA, Lipp E, et al. The genetic landscape of anaplastic astrocytoma. Oncotarget 2014;5:1452–7.
18. Ceccaldi R, Liu JC, Amunugama R, Hajdu I, Primack B, Petalcorin MIR, et al. Homologous-recombination-deficient tumours are dependent on Polθ-mediated repair. Nature 2015;518:258–62.
19. Fujimori H, Hyodo M, Matsuno Y, Shimizu A, Minakawa Y, Atsumi Y, et al. Mismatch repair dependence of replication stress-associated DSB recognition and repair. Heliyon 2019;5:e03057.
20. Supek F, Lehner B, Lindeboom RGH. To NMD or not to NMD: nonsense-mediated mRNA decay in cancer and other genetic diseases. Trends Genet 2021;37:657–68.
21. Lindeboom RGH, Vermeulen M, Lehner B, Supek F. The impact of nonsense-mediated mRNA decay on genetic disease, gene editing and cancer immunotherapy. Nat Genet 2019;51:1645–51.
22. Lykke-Andersen S, Jensen TH. Nonsense-mediated mRNA decay: an intricate machinery that shapes transcriptomes. Nat Rev Mol Cell Biol 2015;16:665–77.
23. Ma Z, Zhu P, Shi H, Guo L, Zhang Q, Chen Y, et al. PTC-bearing mRNA elicits a genetic compensation response via Upf3a and COMPASS components. Nature 2019;568:259–63.
24. Gunn A, Stark JM. I-SceI-based assays to examine distinct repair outcomes of mammalian chromosomal double strand breaks. Methods Mol Biol 2012;920:379–91.
25. Feng W, Simpson DA, Carvajal-Garcia J, Price BA, Kumar RJ, Mose LE, et al. Genetic determinants of cellular addiction to DNA polymerase theta. Nat Commun 2019;10:4286.
26. Yang K, Zhu L, Liu C, Zhou D, Zhu Z, Xu N, et al. Current status and prospect of the DNA double-strand break repair pathway in colorectal cancer development and treatment. Biochim Biophys Acta Mol Basis Dis 2024;1870:167438.
27. Cancer Genome Atlas Network. Comprehensive molecular characterization of human colon and rectal cancer. Nature 2012;487:330–7.
28. Sjöblom T, Jones S, Wood LD, Parsons DW, Lin J, Barber TD, et al. The consensus coding sequences of human breast and colorectal cancers. Science 2006;314:268–74.
29. Fearon ER, Vogelstein B. A genetic model for colorectal tumorigenesis. Cell 1990;61:759–67.
30. Zhao H, Thienpont B, Yesilyurt BT, Moisse M, Reumers J, Coenegrachts L, et al. Mismatch repair deficiency endows tumors with a unique mutation signature and sensitivity to DNA double-strand breaks. Elife 2014;3:e02725.
31. Alexandrov LB, Nik-Zainal S, Wedge DC, Aparicio SAJR, Behjati S, Biankin AV, et al. Signatures of mutational processes in human cancer. Nature 2013;500:415–21.
32. Helleday T, Eshtad S, Nik-Zainal S. Mechanisms underlying mutational signatures in human cancers. Nat Rev Genet 2014;15:585–98.
33. Alexandrov LB, Kim J, Haradhvala NJ, Huang MN, Tian Ng AW, Wu Y, et al. The repertoire of mutational signatures in human cancer. Nature 2020;578:94–101.
34. Roberts SA, Gordenin DA. Hypermutation in human cancer genomes: footprints and mechanisms. Nat Rev Cancer 2014;14:786–800.
35. Kim J, Mouw KW, Polak P, Braunstein LZ, Kamburov A, Kwiatkowski DJ, et al. Somatic ERCC2 mutations are associated with a distinct genomic signature in urothelial tumors. Nat Genet 2016;48:600–6.
36. Vasen HFA, Blanco I, Aktan-Collan K, Gopie JP, Alonso A, Aretz S, et al. Revised guidelines for the clinical management of Lynch syndrome (HNPCC): recommendations by a group of European experts. Gut 2013;62:812–23.
37. Thiagalingam S, Laken S, Willson JK, Markowitz SD, Kinzler KW, Vogelstein B, et al. Mechanisms underlying losses of heterozygosity in human colorectal cancers. Proc Natl Acad Sci U S A 2001;98:2698–702.
38. Liu Y, Sethi NS, Hinoue T, Schneider BG, Cherniack AD, Sanchez-Vega F, et al. Comparative molecular analysis of gastrointestinal adenocarcinomas. Cancer Cell 2018;33:721–35.e8.
39. Zhou J, Gelot C, Pantelidou C, Li A, Yücel H, Davis RE, et al. A first-in-class polymerase theta inhibitor selectively targets homologous-recombination-deficient tumors. Nat Cancer 2021;2:598–610.
40. Rahit KMTH, Tarailo-Graovac M. Genetic modifiers and rare mendelian disease. Genes (Basel) 2020;11:239.
41. El-Brolosy MA, Kontarakis Z, Rossi A, Kuenne C, Günther S, Fukuda N, et al. Genetic compensation triggered by mutant mRNA degradation. Nature 2019;568:193–7.
42. Schimmel J, van Schendel R, den Dunnen JT, Tijsterman M. Templated insertions: a smoking gun for polymerase theta-mediated end joining. Trends Genet 2019;35:632–44.
43. Kent T, Chandramouly G, McDevitt SM, Ozdemir AY, Pomerantz RT. Mechanism of microhomology-mediated end-joining promoted by human DNA polymerase θ. Nat Struct Mol Biol 2015;22:230–7.